Article

Changes in Conformational Dynamics of mRNA upon *At*GRP7 Binding Studied by Fluorescence Correlation Spectroscopy

Mark Schu#ttpelz, Jan C. Scho#ning, So#ren Doose, Hannes Neuweiler, Elisabeth Peters, Dorothee Staiger, and Markus Sauer

J. Am. Chem. Soc., **2008**, 130 (29), 9507-9513 • DOI: 10.1021/ja801994z • Publication Date (Web): 25 June 2008

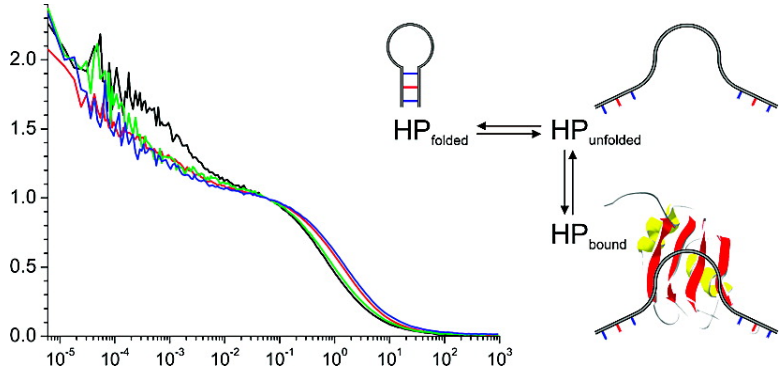

More About This Article

Additional resources and features associated with this article are available within the HTML version:

- Supporting Information
- Access to high resolution figures
- Links to articles and content related to this article
- Copyright permission to reproduce figures and/or text from this article

View the Full Text HTML

J|A|C|S
ARTICLES

Published on Web 06/25/2008

Changes in Conformational Dynamics of mRNA upon *At*GRP7 Binding Studied by Fluorescence Correlation Spectroscopy

Mark Schüttpelz,*,† Jan C. Schöning,‡ Sören Doose,† Hannes Neuweiler,†,§ Elisabeth Peters,†,|| Dorothee Staiger,*,‡ and Markus Sauer*,†

Applied Laser Physics and Laser Spectroscopy, and Molecular Cell Physiology, Bielefeld University, Universitätsstrasse 25, 33615 Bielefeld, Germany

Received March 18, 2008; E-mail: schuettp@physik.uni-bielefeld.de; dorothee.staiger@uni-bielefeld.de; sauer@physik.uni-bielefeld.de

Abstract: The clock-regulated RNA recognition motif (RRM)-containing protein *At*GRP7 (*Arabidopsis thaliana* glycine-rich RNA-binding protein) influences the amplitude of its transcript oscillation at the post-transcriptional level. This autoregulation relies on *At*GRP7 binding to its own pre-mRNA. The sequence and structural requirements for this interaction are unknown at present. In this work, we used photoinduced electron transfer fluorescence correlation spectroscopy (PET−FCS) as a novel technique to study the role of target RNA secondary structure and conformational dynamics during the recognition and binding process. Conformational dynamics of single-stranded (ss) oligonucleotides were studied in aqueous solution with single-molecule sensitivity and high temporal resolution by monitoring fluorescence quenching of the oxazine fluorophore MR121 by guanosine residues. Comparative analysis of translational diffusion constants revealed that both ssRNA and ssDNA bind to *At*GRP7 with similar dissociation constants on the order of 10^{-7} M and that a minimal binding sequence 5′-UUC UGG-3′ is needed for recognition by *At*GRP7. PET−FCS experiments demonstrated that conformational flexibility of short, single-stranded, MR121-labeled oligonucleotides is reduced upon *At*GRP7 binding. In contrast to many other RRM proteins, *At*GRP7 binds to ssRNA preferentially if the RNA is fully stretched and not embedded within a stable secondary structure. The results suggest that *At*GRP7 binding leads to a conformational rearrangement in the mRNA, arresting the flexible target sequence in an extended structure of reduced flexibility that may have consequences for further post-transcriptional processing of the mRNA.

Introduction

Post-transcriptional regulation, including the control of pre-mRNA splicing and maturation as well as mRNA transport, translation, and degradation, critically influences gene expression.[1] Central to these post-transcriptional mechanisms are RNA-binding proteins that, by binding to defined RNA sequences, influence the fate of an mRNA molecule either directly or indirectly through protein−protein interactions.[2,3]

The so-called RNA recognition motif (RRM), or consensus RNA-binding domain (RBD), is one of the most abundant protein domains in eukaryotes. It is defined by two highly conserved ribonucleoprotein (RNP) motifs, the octapeptide RNP1 and the hexapeptide RNP2, in the context of a structurally well-characterized 80 amino acid domain.[4] The RRM fold consists of a four-stranded antiparallel β sheet with two interspersed α helices arranged in the amino acid sequence order $\beta_1\alpha_1\beta_2\beta_3\alpha_2\beta_4$. RNP1 and RNP2 are located in the β_3 and β_1 strands, respectively, and contain conserved aromatic residues that make direct contacts to the RNA substrate.

The N-terminal RRM of human U1A, the A protein of the U1 small nuclear ribonucleoprotein (snRNP), is one of the best-characterized domains.[5,6] It interacts with a 21 nucleotide (nt) stem−loop structure within the U1 small nuclear RNA (snRNA) known as U1 hairpin II (U1hpII). The sequence recognized is a 7 nt single-stranded (ss) region in the loop. In addition, however, U1A has crucial interactions with the loop-closing GC base pair. The ability to bind this heptanucleotide sequence is maintained in different environments [e.g., when it is part of a bulge in the polyadenylation inhibition element, an autoregulatory element in the U1A 3′ untranslated region (UTR)] as long as the key protein−RNA interactions are conserved.[7] The requirement of a double-stranded region of RNA for sequence-specific protein binding has been a general finding for the limited number of known RNA−protein complex structures, although U1A has recently been shown also to have the ability to bind unstructured RNA.[8] On the other hand, some RNA-binding proteins preferentially recognize a single-stranded region of a

† Applied Laser Physics and Laser Spectroscopy.
‡ Molecular Cell Physiology.
§ Current address: MRC Centre for Protein Engineering, Hills Road, Cambridge CB2 0QH, United Kingdom.
|| Current address: Max Planck Institute of Quantum Optics, Hans-Kopfermann-Str. 1, 85748 Garching, Germany.

(1) Moore, M. J. *Science* **2005**, *309*, 1514–1518.
(2) Lorkovic, Z. J.; Wieczorek Kirk, D. A.; Lambermon, M. H.; Filipowicz, W. *Trends Plant Sci.* **2000**, *5*, 160–167.
(3) Olson, S.; Blanchette, M.; Park, J.; Savva, Y.; Yeo, G. W.; Yeakley, J. M.; Rio, D. C.; Graveley, B. R. *Nat. Struct. Mol. Biol.* **2007**, *14*, 1134–1140.
(4) Maris, C.; Dominguez, C.; Allain, F. H. *FEBS J.* **2005**, *272*, 2118–2131.
(5) Hall, K. B.; Stump, W. T. *Nucleic Acids Res.* **1992**, *20*, 4283–4290.
(6) Allain, F. H.; Gubser, C. C.; Howe, P. W.; Nagai, K.; Neuhaus, D.; Varani, G. *Nature* **1996**, *380*, 646–650.
(7) Jovine, L.; Oubridge, C.; Avis, J. M.; Nagai, K. *Structure* **1996**, *4*, 621–631.

target RNA without the assistance of a base-paired stem.[9] For example, the two RRMs of *Drosophila melanogaster* SEX-LETHAL (SXL) protein bind to the polypyrimidine tract at the 3′ splice site of the *transformer* pre-mRNA in an extended conformation with no base pairs and thus block the use of this splice site.[9,10] These different modes of interaction emphasize the importance of secondary structure and conformational dynamics in pre-mRNAs for post-transcriptional events that are induced upon protein binding. Stabilization of hairpin structures or stretched RNA sequences, i.e., reorganization of the RNA structure or arrest in different conformations, by protein binding could be a general mechanism for regulating the fate of the corresponding target mRNA.

In higher plants, the RRM-containing protein *At*GRP7 (*Arabidopsis thaliana* glycine-rich RNA-binding protein) is the prototype of a class of small RNA-binding proteins consisting of a single RRM linked to a glycine-rich C-terminal domain. Oscillations of the *AtGRP7* transcript are controlled by the circadian clock, a key regulator of timed gene expression. The core clockwork comprises proteins which generate their own 24 h oscillation by negative feedback regulation of their own transcription. These molecular oscillators transduce timing information within the cell in order to regulate physiological rhythms. *At*GRP7 is part of a circadian slave oscillator that operates in a clock-output pathway and controls other transcripts.[11,12] In contrast to the core oscillators, *At*GRP7 autoregulates its own expression at the post-transcriptional level through induction of alternative splicing with concomitant decay of the alternatively spliced transcript.[11,13,14] By means of conventional RNA band-shift assays, it was shown that recombinant *At*GRP7 binds to its own transcript.[15] It is conceivable that *At*GRP7 also controls its downstream targets by direct binding. Therefore, identification of a minimal binding sequence and the influence of RNA secondary structure would contribute to the identification of target transcripts.

Since its introduction in the 1970s, fluorescence correlation spectroscopy (FCS)[16] has been successfully used to study molecular interactions between biomolecules at the single-molecule level.[17–20] FCS provides information about molecular dynamic processes by analyzing fluctuations in the signal arising from fluorescent molecules as they pass the observation volume. Therefore, it can be used to gain information on any process(es) affecting the fluorescence intensity, e.g., translational diffusion, photophysical processes, or intermolecular interactions. FCS binding studies usually require a small fluorescent receptor whose diffusion constant changes upon binding to a considerably larger nonfluorescent ligand. In combination with intramolecular quenching interactions such as Förster resonance energy transfer (FRET) or alternative quenching interactions, FCS has become an established tool for monitoring conformational dynamics of flexible biopolymers, providing rate constants directly from amplitudes and characteristic decay times of FCS curves.[21–24]

It is known that the fluorescence of several oxazine and rhodamine fluorophores is selectively quenched upon van der Waals contact with guanosine or tryptophan.[22–27] This photo-induced electron transfer (PET)-based quenching mechanism lays the foundation for a method with single-molecule sensitivity that allows probing of conformational changes in macromolecules through a reporter fluorophore that is in a fluorescent or nonfluorescent state depending on the proximity of a quencher molecule.[23,24] The system's two-state nature, with its absence of intermediate intensity values, simplifies the data analysis and, in particular, allows straightforward interpretation of the correlation analysis.

In this work, we used PET−FCS to investigate the binding properties of *At*GRP7, employing synthetic oligoribonucleotides (ORNs) and oligodeoxyribonucleotides (ODNs) as binding substrates. We first revealed the critical nucleic acid residues of the *At*GRP7 target sequence using FCS binding experiments on short, overlapping, fluorescently labeled ODN sequences. Furthermore, we studied the binding of *At*GRP7 to single- and double-stranded target sequences. Results of PET−FCS studies employing RNA hairpins as the target sequence in the loop with flanking stems of different stabilities reveal changes of their conformational flexibility upon *At*GRP7 binding. We therefore conclude that the flexible mRNA binding sequence is arrested in an extended stretched conformation.

Experimental Section

Synthesis of Fluorescently Labeled Oligonucleotides. Synthetic DNA and RNA oligonucleotides were purchased from IBA (Göttingen, Germany) and biomers.net (Ulm, Germany). The oxazine derivative MR121 was kindly provided by K. H. Drexhage (University of Siegen). Oligonucleotides were labeled with MR121 at the amino-modified 5′ or 3′ terminus via an aliphatic C3 or C6 amino modifier using *N*-hydroxysuccinimidyl ester chemistry. Labeling and purification were performed as described previously.[23]

Protein Expression. The expression plasmid encoding the glutathione S-transferase (GST)−*At*GRP7 fusion protein has been described.[15] An N-terminal sequence of 101 amino acids constituting the RRM of U1A was amplified from the plasmid HA-hU1A: pQE30.1 (kindly provided by C. Kambach from PSI, Villigen, Switzerland) and fused in frame to GST in the vector pGEX-6P-1 (GE Healthcare, Freiburg, Germany). Recombinant proteins were expressed in *Escherichia coli* BL21 and purified from crude lysates using batch absorption on glutathione agarose, as described

(8) Law, M. J.; Rice, A. J.; Lin, P.; Laird-Offringa, I. A. *RNA* **2006**, *12*, 1168–1178.
(9) Handa, N.; Nureki, O.; Kurimoto, K.; Kim, I.; Sakamoto, H.; Shimura, Y.; Muto, Y.; Yokoyama, S. *Nature* **1999**, *398*, 579–585.
(10) Banerjee, H.; Rahn, A.; Davis, W.; Singh, R. *RNA* **2003**, *9*, 88–99.
(11) Heintzen, C.; Nater, M.; Apel, K.; Staiger, D. *Proc. Natl. Acad. Sci. U.S.A.* **1997**, *94*, 8515–8520.
(12) Schöning, J. C.; Streitner, C.; Staiger, D. *Biol. Rhythm Res.* **2006**, *37*, 335–352.
(13) Staiger, D.; Apel, K. *Mol. Gen. Genet.* **1999**, *261*, 811–819.
(14) Rudolf, F.; Wehrle, F.; Staiger, D. *Biochemist* **2004**, *26*, 11–13.
(15) Staiger, D.; Zecca, L.; Wieczorek Kirk, D. A.; Apel, K.; Eckstein, L. *Plant J.* **2003**, *33*, 361–371.
(16) Magde, D.; Elson, E. L.; Webb, W. W. *Biopolymers* **1974**, *13*, 29–61.
(17) Eigen, M.; Rigler, R. *Proc. Natl. Acad. Sci. U.S.A.* **1994**, *91*, 5740–5747.
(18) Schwille, P.; Bieschke, J.; Oehlenschlager, F. *Biophys. Chem.* **1997**, *66*, 211–228.
(19) Chen, Y.; Muller, J. D.; Tetin, S. Y.; Tyner, J. D.; Gratton, E. *Biophys. J.* **2000**, *79*, 1074–1084.
(20) Hess, S. T.; Huang, S.; Heikal, A. A.; Webb, W. W. *Biochemistry* **2002**, *41*, 697–705.
(21) Chattopadhyay, K.; Elson, E. L.; Frieden, C. *Proc. Natl. Acad. Sci. U.S.A.* **2005**, *102*, 2385–2389.
(22) Neuweiler, H.; Doose, S.; Sauer, M. *Proc. Natl. Acad. Sci. U.S.A.* **2005**, *102*, 16650–16655.
(23) Kim, J.; Doose, S.; Neuweiler, H.; Sauer, M. *Nucleic Acids Res.* **2006**, *34*, 2516–2517.
(24) Doose, S.; Neuweiler, H.; Barsch, H.; Sauer, M. *Proc. Natl. Acad. Sci. U.S.A.* **2007**, *104*, 17400–17405.
(25) Knemeyer, J. P.; Marme, N.; Sauer, M. *Anal. Chem.* **2000**, *72*, 3717–3724.
(26) Neuweiler, H.; Schulz, A.; Bohmer, M.; Enderlein, J.; Sauer, M. *J. Am. Chem. Soc.* **2003**, *125*, 5324–5330.
(27) Doose, S.; Neuweiler, H.; Sauer, M. *ChemPhysChem* **2005**, *6*, 2277–2285.

elsewhere.[28] The *At*GRP7 moiety was released from the glutathione agarose column by PreScission protease (GE Healthcare, Freiburg, Germany) cleavage, and the solution was concentrated by centrifugation through Centricon filter devices (Millipore).

Fluorescence Correlation Spectroscopy. FCS experiments were performed on a custom-made confocal fluorescence microscope as described previously.[22] Fluorescently labeled oligonucleotides were diluted to a final concentration of ~0.5 nM in phosphate-buffered saline (PBS, pH 7.4) containing 0.3 mg/mL bovine serum albumin (BSA) and 0.05% Tween-20 to suppress glass-surface interactions. Unless otherwise stated, a 1000-fold excess of *At*GRP7 was used. Excitation intensities were adjusted to 500 μW at the back aperture of the objective in order to avoid possible artifacts due to photobleaching and fluorescence saturation of the fluorophore. For measurements with ORNs, the ribonuclease inhibitor RiboLock (Fermentas, St. Leon-Rot, Germany) (400 units/mL) and tRNA (10 μg/mL) were added to the buffer. FCS measurements were carried out in 100 μL of solution enclosed by a recessed slide and a coverslip. Alternatively, perforated silicone sheets (Invitrogen, Karlsruhe, Germany) covered by two coverslips were used for sample volumes of a few microliters. All of the measurements were performed at room temperature.

PET quenching interactions lead to on/off fluctuations in the fluorescence signal and can be analyzed as described previously.[23] In this work, the correlation function $G(\tau)$ of the fluorescence fluctuations of N molecules freely diffusing through the excitation and detection volume with a characteristic diffusion time τ_D was analyzed by fitting a two-dimensional diffusion model that included a stretched-exponential term to account for quenching dynamics:

$$G(\tau) = \frac{1}{N}\left(1 + \frac{\tau}{\tau_D}\right)^{-1}\left[1 + Ke^{-(\tau/\tau_K)^{\beta}}\right] \quad (1)$$

Here, the characteristic diffusion time is $\tau_D = \omega_{xy}^2/4D$, where ω_{xy} is the lateral radius of the excitation and detection volume; D is the diffusion coefficient, given by the Stokes−Einstein equation $D = k_BT/6\pi\eta R$, where T is the temperature, η is the viscosity of the medium, R is the hydrodynamic radius, and k_B is Boltzmann's constant; and K, τ_K, and β are the amplitude, relaxation time, and stretch parameter, respectively, for the stretched-exponential decay. To obtain an approximation of R, a molecule with molecular weight M_r can be described as a homogeneous sphere with a mean density ρ:

$$R = \left(\frac{3M_r}{4\pi\rho N_A}\right)^{1/3} \quad (2)$$

where N_A is Avogadro's constant. R is therefore proportional to the cube root of the molecular weight. From the stretched-exponential decay constants β, τ_K, and K, a mean relaxation time $\langle\tau\rangle$ and the rate constants k_{AB} and k_{BA} for transitions between the fluorescent state (A) and the nonfluorescent state (B) can be calculated using the following expressions:[23]

$$\langle\tau\rangle = \frac{\tau_K}{\beta}\Gamma\left(\frac{1}{\beta}\right) \quad (3)$$

$$k_{AB} = \frac{K}{\langle\tau\rangle(K+1)} \qquad k_{BA} = \frac{1}{\langle\tau\rangle(K+1)} \quad (4)$$

where $\Gamma(x)$ is the gamma function.

Results and Discussion

Identification of Critical Residues for Binding on the *At*GRP7 Target Sequence. Previous studies have shown that *At*GRP7 binds to the 32 nt sequence 5′-AUU UUG UUC UGC UUC UGG UUU AGA UUU GAU GU-3′ located in the 3′ UTR of its mRNA.[15,28] To study mRNA binding in more detail, we performed FCS experiments with various oligonucleotides labeled at the 5′ end with the red-absorbing fluorophore MR121. The first of these experiments studied binding of recombinant *At*GRP7 to the ORN 7-UTR_WT, representing the 32 nt binding site in the 3′ UTR (Figure 1).[28]

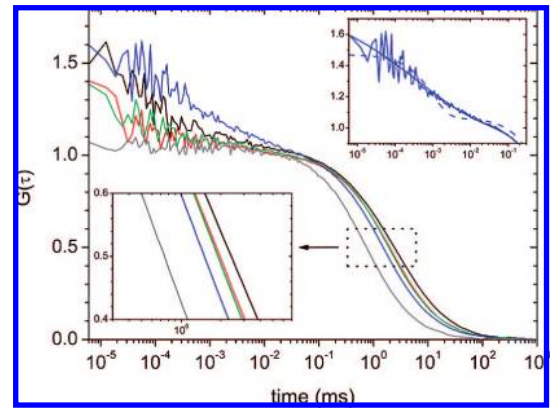

Figure 1. Fluorescence correlation functions $G(\tau)$ of 10^{-9} M aqueous solutions of the MR121-labeled ORN 7-UTR_WT in the absence (blue) and presence (black) of recombinant *At*GRP7 and of 7-UTR_WT hybridized to a complementary oligodeoxynucleotide in the absence (green) and presence (red) of *At*GRP7. For comparison, the correlation function obtained from a short ODN [MR121-$(T)_{10}$] without G residues (gray) is also shown. All of the FCS curves were normalized to the number of observed fluorophores. Diffusion through the excitation and detection volume takes place on the millisecond time scale (see the inflection point magnified in the lower-left inset). Whereas FCS data for oligonucleotides without G residues are well-described by a simple diffusion model, all other oligonucleotides containing several G residues show an additional amplitude on the nanosecond-to-microsecond time scale that can only be fitted with comparable accuracy using a stretched-exponential function (continuous line) instead of a monoexponential function (dashed line) (see the upper-right inset).

Freely diffusing MR121-labeled ORN 7-UTR_WT exhibited a characteristic diffusion time τ_D of 1.49 ms (the standard deviations estimated from three measurements were less than 0.1 ms) that increased 1.6-fold (τ_D = 2.39 ms) when bound to *At*GRP7. An RNA/DNA hybrid consisting of the ORN 7-UTR_WT and the complementary ODN exhibited a τ_D of 1.92 ms that remained unchanged upon addition of *At*GRP7, demonstrating that this protein does not bind to the target sequence when the target is presented as a double strand. Furthermore, *At*GRP7 did interact with a single-stranded ODN representing the 32 nt target sequence 5′-ATT TTG TTC TGG TTC TGC TTT AGA TTT GAT GT-3′. Titrations of the MR121-labeled 32 nt ORN and ODN with *At*GRP7 yielded dissociation constant (K_d) values of 4.89×10^{-7} and 1.02×10^{-7} M for the ORN and the ODN, respectively (the standard deviations were less than 1×10^{-7} M for all of the K_d measurements). The slightly stronger binding of *At*GRP7 to the ssODN can be explained either by stronger binding to DNA or by the reduced tendency of ODNs to form secondary structures, as evidenced by the longer diffusion time for the pure MR121-labeled ssODN than for the ssORN (1.77 and 1.56 ms, respectively), which reflects a larger hydrodynamic radius.

The ability of many RRM-containing proteins to recognize both ssDNA and ssRNA has previously been noted. For example, the specificity of recombinant human hnRNP A1, a major constituent of heterogeneous nuclear RNPs, is mimicked in ssODNs,[29] and hnRNP A1 binds with approximately equal affinities to both telomeric DNA and its RNA analogue.[30]

For in vitro experiments, DNA offers several advantages, such as increased stability for chemical-labeling reactions and long-

(28) Schöning, J. C.; Streitner, C.; Page, D. R.; Hennig, S.; Uchida, K.; Wolf, E.; Furuya, M.; Staiger, D. *Plant J.* **2007**, *52*, 1119–1130.

Table 1. Dissociation Constants (K_d) for Binding between *At*GRP7 and Overlapping DNA Oligonucleotides Scanning the 3′ UTR Target Site

ODN	DNA oligonucleotide sequence	K_d (10^{-7} M)[a]
7-UTR_WT	5′-ATT TTG TTC TGG TTC TGC TTT AGA TTT GAT GT-3′	1.0
1	5′-CT ATT TTG TTC T-3′	≥11.0
2	5′-ATT TTG TTC TGG-3′	2.7
3	5′-T TTG TTC TGG TT-3′	2.4
4	5′-TG TTC TGG TTC T-3′	3.7
5	5′-TTC TGG TTC TGC-3′	1.9
6	5′-C TGG TTC TGC TT-3′	4.3
7	5′-GG TTC TGC TTT A-3′	≥10.0
8	5′-TTC TGC TTT AGA-3′	≥8.5

[a] Standard deviations are less than 1×10^{-7} M for all measurements.

term measurements. Therefore, we used ODNs to identify critical residues on the *At*GRP7 target sequence. A 15-mer ODN representing the 5′ half of 7-UTR_WT strongly interacted with *At*GRP7, whereas a 17-mer representing the 3′ half did not show significant binding (data not shown). We then synthesized overlapping 12-mer ODNs derived from the 5′ half and determined their K_d values from the characteristic diffusion times in FCS experiments (Table 1). Shifting the 12 nt sequence from the 5′ end of the native 32 nt sequence caused the binding strength to increase considerably upon incorporation of two G residues (compare the K_d values for ODNs 1 and 2). Furthermore, the binding efficiency decreased upon removal of two T residues near the 5′ end (compare the K_d values for ODNs 5 and 6). Upon removal of additional residues from the 5′ end, the binding strength gradually decreased (compare the K_d values for ODNs 6, 7, and 8). These observations lead to the conclusion that the two T residues at the 5′ end of ODN 5 and the two G residues at the 5′ end of ODN 7 are important for *At*GRP7 binding, thereby identifying 5′-TTC TGG-3′ as the critical binding sequence. This is in line with our previous observations that poly(G) and poly(U) ribohomopolymers compete for *At*GRP7 binding to the 3′ UTR[15] and that mutation of several G residues within the 7-UTR_WT ORN weakens binding.[28]

Changes in Conformational Dynamics of mRNA upon Binding to *At*GRP7. In addition to analysis of translational diffusion, PET−FCS allows direct monitoring of RNA conformational dynamics. Dynamics of intramolecular contact formation are reported by the association/dissociation kinetics of MR121 and guanosine residues.[23] Fluctuations in fluorescence intensity induced by MR121−G complex formation/dissociation lead to the appearance of a quenching amplitude in the nanosecond-to-microsecond time range that can be analyzed using eq 1. Because formation of nonfluorescent MR121−G complexes results in fluorescence fluctuations between on and off states that depend on the conformational flexibility of the oligonucleotide, association (i.e., contact formation) and dissociation rates as well as the equilibrium distribution could be calculated by applying a two-state model. The absence of photophysics, i.e., intersystem crossing of the fluorophore leading to additional fluctuations in the nanosecond-to-microsecond time range, was confirmed by the flat FCS curve measured for an MR121-labeled ODN without G residues (see the gray curve in Figure 1).

All G-containing ORNs and ODNs show pronounced fluorescence fluctuations on the nanosecond-to-microsecond time scale due to contact-induced quenching mediated by the conformational dynamics of the oligonucleotides. Whereas the FCS data for ODNs containing a single G can be well-described by a monoexponential decay function,[23] the presence of several G residues in the ORN 7-UTR_WT significantly altered the decay, which required a description in terms of a stretched-exponential function (see the upper-right inset of Figure 1). The stretched-exponential decay reflects fluorescence fluctuations on different time scales caused by contact formation with G residues located at different positions in the ORN. Upon hybridization of the ORN to the complementary ODN, the quenching fluctuations were strongly diminished (compare the blue and green curves in Figure 1). This demonstrates that contact formation between MR121 and G is reduced as a result of the increased rigidity in double-stranded as opposed to single-stranded oligonucleotides, as expected.

The fluorescence fluctuations of MR121-labeled ORN 7-UTR_WT changed upon *At*GRP7 binding (compare the blue and black curves in Figure 1). Fluorescence quenching of MR121 by G via PET was reduced, indicating a conformational reorganization imposed by protein binding. In particular, the ORN exhibited fluorescence fluctuations on different time scales resulting from formation of contacts with different G residues located at different positions in the oligonucleotide. If it is assumed that the conformational dynamics of such a heterogeneous system can still be described by a two-state conformational fluctuation model with open and closed states, the fluorescence quenching fluctuations (PET−FCS) can be used in addition to standard diffusion analysis (FCS) to characterize binding.

To quantify the distribution of fluorescence fluctuations in PET−FCS curves caused by formation of contacts between the MR121 fluorophore and different guanosine residues, a stretched-exponential model (eq 1) was required.[31] In this model, the stretch parameter β describes the heterogeneity of the system: a smaller value of β corresponds to a broader distribution of transition rate constants. In the following PET−FCS experiments, we used the 12 nt ODN 3, which contains three G residues (Table 1). PET−FCS curves obtained at different *At*GRP7 concentrations were analyzed using a constant β value of 0.4, which enabled reliable and numerically stable fitting for all protein concentrations. Values of the characteristic diffusion

(29) Buvoli, M.; Cobianchi, F.; Biamonti, G.; Riva, S. *Nucleic Acids Res.* **1990**, *18*, 6595–6600.
(30) Abdul-Manan, N.; O'Malley, S. M.; Williams, K. R. *Biochemistry* **1996**, *35*, 3545–3554.
(31) Lindsey, C. P.; Patterson, G. D. *J. Chem. Phys.* **1980**, *73*, 3348–3357.

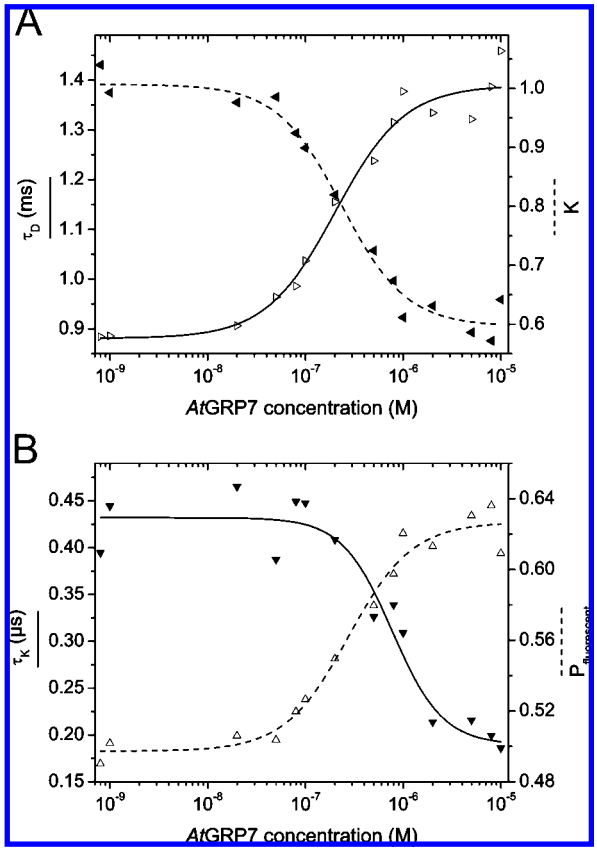

Figure 2. Sigmoidal binding isotherms for the fluorescence correlation function parameters (A) τ_D (solid curve) and K (dashed curve) and (B) τ_K (solid curve) and $P_{\text{fluorescent}}$ (dashed curve), obtained from PET−FCS measurements at an excitation power of 500 μW for the titration of MR121-labeled ODN 3 with *At*GRP7.

time (τ_D), the equilibrium constant for the fluorescence quenching kinetics (K = [B]/[A]), the corresponding fraction of fluorescent oligonucleotides {$P_{\text{fluorescent}}$ = [A]/([A] + [B]) = 1/(1 + K)}, and the characteristic relaxation time for the quenching process (τ_K) were plotted against the *At*GRP7 concentration (Figure 2A, B). All of the titration curves revealed the existence of two states, representing the free and bound states of the oligonucleotide. From the sigmoidal binding isotherms in Figure 2, the following dissociation constant values (each labeled with a superscript indicating the curve used) were determined: $K_d^{\tau_D} = 2.02 \times 10^{-7}$ M, $K_d^{K} = 2.25 \times 10^{-7}$ M, $K_d^{P_{\text{fluorescent}}} = 2.75 \times 10^{-7}$ M, and $K_d^{\tau_K} = 7.73 \times 10^{-7}$ M. These values show good agreement with each other, with only $K_d^{\tau_K}$ being larger by a factor of 3. As Figure 2B shows, τ_K decreased with increasing *At*GRP7 concentration. This is indicative of changes in the conformational flexibility of the oligonucleotide upon protein binding that reduce formation of quenching contacts between MR121 and G residues. Simultaneously, the fraction of fluorescent oligonucleotides increased.

To retrieve more details about the conformational changes induced upon protein binding, we used eqs 3 and 4 to calculate the association rate constant k_{AB} and the dissociation rate constant k_{BA} for contact-induced quenching of MR121 by G. Whereas association and dissociation occurred with similar efficiency [$k_{AB} \approx k_{BA} = (0.3-0.4) \times 10^6$ s^{-1}] for low protein concentrations (10^{-9} M), both rates increased with increasing protein concentration. In principle, association and dissociation rates can be determined from the stretched-exponential model. However, because of the complex distribution of the fluorescence fluctuations, these rates are very difficult to interpret. The dissociation rate constant is expected to be independent of protein concentration, as it is controlled by MR121−G interactions, whereas the experimental results demonstrate that it is altered by protein binding. The values of k_{AB} and k_{BA} increased to 0.6×10^6 and 1.0×10^6 s^{-1}, respectively, at an *At*GRP7 concentration of 10^{-5} M. The increase in k_{AB} can also be explained in terms of protein binding, which restricts the conformational space of the oligonucleotide, resulting in an increased association rate.

Table 2. RNA Hairpins Used in *At*GRP7 Binding Experiments

label	RNA oligonucleotide sequence[a]	ΔG (kcal/mole)[b]
NT[c]	5′-U UUG **UUC UGG** UUC-3′	1.0
HP	5′-*G UG*G **UUC UGG** *CAC*-3′	−1.8
HP_{UA}	5′-*GU UG*G **UUC UGG** *CAA* C-3′	−3.0
HP_{GC}	5′-*GG UG*G **UUC UGG** *CAC* C-3′	−5.2
HP_{2GC}	5′-*GGG UGG* **UUC UGG** *CAC CC*-3′	−8.6

[a] The *At*GRP7 binding sequence is shown in bold characters; point mutations and additional nucleotides are shown in italics, and stem-forming nucleotides are underlined. [b] Gibbs free energy for hairpin formation at 20 °C and a sodium concentration of 140 mM.[32] [c] Native (nonhairpin) ORN.[28]

Influence of RNA Secondary Structure on *At*GRP7 Binding. The effect of conformational flexibility of the RNA target sequence on protein binding efficiency has not been entirely resolved. To study the *At*GRP7 binding mechanism in more detail, we designed RNA hairpins exposing the core binding sequence 5′-UUC UGG-3′ in a loop. By insertion of point mutations in the native sequence and addition of nucleotides at the 3′ and 5′ ends, artificial stems consisting of 3−5 base pairs (HP, HP_{UA}, HP_{GC}, and HP_{2GC}; Table 2) were formed. Because MR121 was coupled to the 3′ end, efficient quenching by G residues in the 5′ terminal stem could take place only in the closed RNA hairpins. Fluorescence-intensity melting curves (Figure S1 in the Supporting Information) showed an increase in melting temperature corresponding to the increase in Gibbs free energies predicted using MFOLD,[32] thus corroborating the formation of RNA hairpins in HP, HP_{UA}, HP_{GC}, and HP_{2GC}. In their closed states, the hairpins showed reduced fluorescence intensities, with fluorescence quantum yields of 0.38 for HP, 0.22 for HP_{UA}, and 0.13 for both HP_{GC} and HP_{2GC} relative to the free fluorophore.

Figure 3 shows FCS curves for the native (i.e., extended) ORN NT and the hairpin ORN HP in the absence and presence of *At*GRP7. Although the characteristic diffusion times of the two ORNs were quite similar, the fluorescence quenching revealed by the PET amplitude in the nanosecond-to-microsecond time range showed significant differences. In particular, the RNA hairpins exhibited efficient quenching by G residues in the complementary stem, resulting in more-pronounced fluorescence quenching amplitudes in the PET−FCS curves. Addition of *At*GRP7 caused the formation of RNA/protein complexes, as reflected in increased diffusion times. Titration curves of FCS diffusion times yielded the dissociation constant values $K_d^{HP} = 5.7 \times 10^{-7}$ M and $K_d^{NT} = 2.4 \times 10^{-7}$ M for the HP and native NT ORNs, respectively, in agreement with the value for the 12-mer ODN 3 (Table 1) and confirming that *At*GRP7

(32) Zuker, M.; Mathews, D. H.; Turner, D. H. In *RNA Biochemistry and Biotechnology*; Barciszewski, J., Clark, B. F. C., Eds.; Kluwer Academic Publishers: Dordrecht, The Netherlands, 1999, p 11−43.

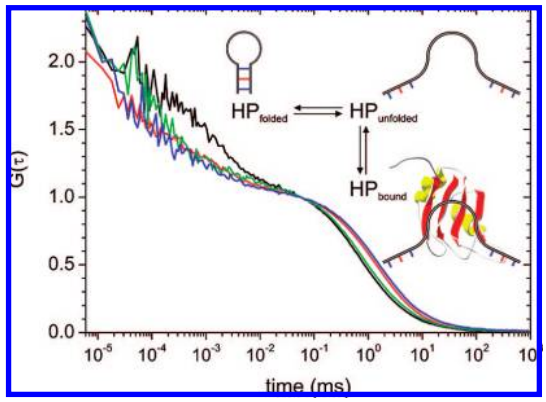

Figure 3. Normalized FCS curves measured for 10^{-9} M solutions of the RNA hairpin HP and the native ORN NT in the absence and presence of *At*GRP7 protein. The fluorescence correlation functions of free HP and NT are shown in black and green, respectively. The curve for HP bound to *At*GRP7 is shown in red and that for NT bound to *At*GRP7 in blue. The proposed model of a two-state hairpin-folding equilibrium whose unfolded state can be bound by the protein[33] is illustrated in the inset.

binds with similar affinities to ssRNA and ssDNA. Furthermore, our findings indicate that the efficiency of *At*GRP7 binding is only slightly reduced when the target sequence is exposed in the loop of an RNA hairpin and demonstrate that the mutations introduced to generate the flanking stem had no significant influence on the binding efficiency.

The FCS curves measured for the free ORNs NT and HP exhibited different decays in the nanosecond-to-microsecond time range, whereas those in the presence of *At*GRP7 protein appeared to be similar (Figure 3). For both ORNs, the correlation amplitudes of the microsecond decay decreased upon *At*GRP7 binding, reflecting reduced quenching of MR121 due to complex formation with G. The similarity of the two curves under conditions of bound protein demonstrates that the MR121 fluorophore experienced identical environments, i.e., the nearest quenching G residues were located at least three nucleotides apart (compare the ORN sequences in Table 2). This implies that the hairpin structure was disrupted.

To further examine the influence of the hairpin stem on *At*GRP7 binding, the RNA hairpin structure was stabilized by incorporation of additional base pairs into the stem. The resulting RNA hairpins HP_{UA} and HP_{GC} (with stems containing four base pairs) and the hairpin HP_{2GC} (with five base pairs in the stem) exhibited higher melting temperatures and smaller fluorescence intensities (Figure S1 in the Supporting Information). FCS curves recorded in the absence and presence of an excess of *At*GRP7 demonstrated that the binding efficiency decreased with increasing hairpin stability (Figure S2 in the Supporting Information). Binding was probed by comparison of the diffusion times in the absence and presence of 10^{-6} M *At*GRP7. Whereas HP_{UA}, with one additional UA base pair, showed protein binding, the slightly more stable HP_{GC} exhibited severely reduced binding. The most stable hairpin, HP_{2GC} (with five base pairs in the stem), showed no *At*GRP7 binding at all (Figure S2C in the Supporting Information). To compare the behavior of *At*GRP7 with that of an RNA−protein interaction for which the secondary structure is known, we performed FCS experiments on a synthetic 3′-labeled RNA hairpin derived from the U1A binding ORN U1hpII (5′-AAU CCA UUG CAC UCC GGA UUU-3′) in the presence of increasing concentrations of recombinant U1A protein (Figure S3 in the Supporting Information). U1A efficiently binds to this relatively stable RNA hairpin, which has five base pairs in the stem. Analysis of the diffusion times measured at different protein concentrations revealed a sigmoidal binding curve and a K_d value of 6×10^{-10} M, which is in good agreement with literature values for interaction of U1A with its targets.[5,8,34] These observations clearly demonstrate that *At*GRP7 only binds to these ssORNs in an extended conformation. It is known that DNA and RNA hairpins form a dynamic equilibrium between open (extended) and closed conformations that includes several intermediate trap states.[23,35] The kinetics of transitions between the different conformational states depends on the numbers of nucleotides in the loop and the stem and their ratio as well as on experimental conditions such as ionic strength and temperature.

Given the conformational dynamics of RNA, it follows that the ORNs HP and HP_{UA} fluctuate between open and closed conformations and that *At*GRP7 protein selectively binds to the open conformation, arresting the RNA in its extended structure (as illustrated in the inset of Figure 3). In other words, HP and HP_{UA} present a high proportion of ORNs in extended conformations, ensuring efficient binding of the protein. On the other hand, rather stable hairpins such as HP_{GC} and HP_{2GC} do not provide enough possibilities for efficient *At*GRP7 binding, i.e., conformations with the extended RNA recognition sequence are available less frequently as a result of increased hairpin stability. Thus, our results imply that the structure of the *At*GRP7 recognition sequence in the 3′ UTR fluctuates between different closed and open conformations as well as intermediate ones. The influence of secondary structure modification on biological function has been demonstrated for the HuR protein.[36] Binding of HuR to single-stranded AU-rich elements, which determine mRNA half-life, protects the mRNAs from degradation. Addition of artificial mRNA openers enhanced the HuR function whereas specific closers blocked the HuR binding and induced mRNA decay in a cell lysate system.[36] Likewise, *At*GRP7 binding to the pre-mRNA arrests the structure in an extended conformation and might initiate different processing mechanisms, such as alternative splicing and RNA degradation. Structural flexibility of RNA and protein-induced adjustment in a specific conformation might be common features of protein recognition and post-transcriptional mRNA processing. Our results are strengthened by recent studies of the binding of different DNA ligands to the anti-ssDNA antigen-binding fragment DNA-1.[37] X-ray crystallography revealed that the conformation of the bound ligand differs from the predicted hairpin conformation. In fact, our measurements clearly demonstrate that *At*GRP7 binds preferentially to RNA in a single-stranded conformation whereby a conformational reorganization of the mRNA sequence is triggered.

Conclusions

In this work, we studied binding-site requirements for the single RRM-containing protein *At*GRP7. Initially, we used standard FCS analysis to identify a minimal *At*GRP7 binding site (5′-UUC UGG-3′) within the known 32 nt sequence of its

(33) Guex, N.; Peitsch, M. C. *Electrophoresis* **1997**, *18*, 2714–2723.
(34) Lutz-Freyermuth, C.; Query, C. C.; Keene, J. D. *Proc. Natl. Acad. Sci. U.S.A.* **1990**, *87*, 6393–6397.
(35) Van Orden, A.; Jung, J. *Biopolymers* **2008**, *89*, 1–16.
(36) Meisner, N. C.; Hackermuller, J.; Uhl, V.; Aszodi, A.; Jaritz, M.; Auer, M. *ChemBioChem* **2004**, *5*, 1432–1447.
(37) Ou, Z.; Bottoms, C. A.; Henzl, M. T.; Tanner, J. J. *J. Mol. Biol.* **2007**, *374*, 1029–1040.

3′ UTR. Our results showed that *At*GRP7 binds both ssDNA and ssRNA with comparable efficiencies. Exploiting selective fluorescence quenching of MR121 by guanosine residues, PET−FCS demonstrated that the conformational flexibility of the mRNA target sequence is significantly reduced upon *At*GRP7 binding. These findings suggest that *At*GRP7 exerts post-transcriptional control by arresting the mRNA in a state with restricted conformational dynamics. RNA hairpins that provide the binding sequence in the loop and have stems containing up to four base pairs were substantially destabilized upon binding of *At*GRP7. However, *At*GRP7 did not bind to RNA hairpins stabilized by more than four base pairs in the stem. These results demonstrate that in contrast to many other RNA-binding proteins but similar to *D. melanogaster* SXL protein, *At*GRP7 binds to RNA only if the RNA is not embedded within a secondary structure. In other words, *At*GRP7 binding reduces conformational dynamics by arresting the flexible binding sequence in a stretched conformation. Trapping of a pre-mRNA in a defined secondary structure could be a general mechanism for triggering alternative processing.

Acknowledgment. We thank K. H. Drexhage for providing MR121 and E. Detring for isolating recombinant proteins. We are indebted to C. Kambach for making available the HA-hU1A: pQE30.1 clone and for helpful discussions. J.C.S. is a fellow of the German National Academic Foundation. The work was funded by the German Research Foundation (SFB613, STA653/2).

Supporting Information Available: Melting curves for the RNA hairpins HP, HP_{UA}, HP_{GC}, and HP_{2GC} and FCS curves from hairpin−*At*GRP7 and hairpin−U1A binding studies. This material is available free of charge via the Internet at http://pubs.acs.org.

JA801994Z